Theoretical and Experimental Investigation of Interfacial Instabilities in Coextrusion Feed-Block Dies

Modified on Monday, 27 April 2015 09:16 PM by mpieler — Categorized as: Paper of the Month

Theoretical and Experimental Investigation of Interfacial Instabilities in Coextrusion Feed-Block Dies

M. Zatloukal[1], A. Xue[2], M. Amon[2]

[1]Polymer Centre, Faculty of Technology, Tomas Bata University in Zlin, Zlin, Czech Republic
[2]Avery Dennison Corporation, Painesville, USA

Abstract

In this work, wave type of interfacial instabilities occurring during the coextrusion process have been investigated by using different feedblock geometries and polymers. It has been found that the onset of interfacial instabilities can be captured by the quantification of the stretching discontinuity occurring on the interface between different polymers.

Introduction

Interfacial instabilities represent internal distortions occurring on the interface during coextrusion processes which can negatively influence optical and mechanical properties of the final product [1]. It has been found that the onset of interfacial instabilities can be captured through evaluation of the layer stretching at the interface by using so called Total Normal Stress Difference (TNSD), Principle Stress Difference (PSD) or Flow Direction Normal Stress (FDNS) [2-12]. In this work, specific attention will be paid to wave type of interfacial instabilities (having high amplitude and low frequency) which occurs during coextrusion process by using feedblock dies. Two feedblock geometries (with different merging areas) and polymers with different level of extensional strain hardening were considered to evaluate the role of polymer melt rheology on the flow stability.

Experimental

Materials
In this work, three different polyolefin blends (FCC, FCS1 and FCS2) have been used during coextrusion experiments.

Rheological measurements
Uniaxial extensional viscosity at low extensional rates was measured using ARES equipped by the SER Universal Testing Platform (SER-HV-A01 model) from Xpansion Instruments [13-14] whereas twin bore Rosand RH7-2 control speed capillary rheometer has been used to determine shear and uniaxial extensional viscosity at high deformation rates by using Cogswell model. The measured rheological data for corresponding samples are provided in Figures 1-4.

Coextrusion experiment
Experimental work has been done on two different feedblock geometries (see Figures 5-6) at different processing conditions which are summarized in Table 1.

Mathematical Modeling

Non-isothermal viscoelastic steady state two dimensional Finite Element Method (FEM) simulations were performed by solving the well-known mass, momentum and energy equations using the commercially available Compuplast software VEL 6.3. In this study, the modified Leonov constitutive equation is employed. The constitutive equation is based on the original Leonov model [15] with modified dissipation term, b, proposed by Zatloukal [16]. The relation between stress and elastic strain is given by

$$\tau = 2\left(c\frac{\partial W}{\partial I_1} - c^{-1}\frac{\partial W}{\partial I_2} \right) \qquad (1)$$

where τ is the stress tensor and W denotes elastic potential depends on the invariant I_1 and I_2 of the recoverable Finger tensor. Elastic potential is defined by

$$W = \frac{3G}{2(n+1)}\left\{ (1-\beta)\left[\left(\frac{I_1}{3} \right)^{n+1} - 1 \right] + \beta\left[\left(\frac{I_2}{3} \right)^{n+1} - 1 \right] \right\} \qquad (2)$$

where G is the linear elastic modulus, β and n are nonlinear parameters. In this work, both non-linear parameters β and n were adjusted to be zero. Dissipation term, b, is included in irreversible rate of strain equation, e_p

$$e_p = b\left[c - \left(\frac{I_1}{3} \right)\delta \right] - b\left[c^{-1} - \left(\frac{I_2}{3} \right)\delta \right] \qquad (3)$$

where δ stands for the unit tensor. The Elastic strain is related to the deformation history as

$$\overset{0}{c} - c \cdot D - D \cdot c + 2c \cdot e_p = 0 \ . \qquad (4)$$

Here, D denotes the rate of deformation tensor. Modified dissipation term, b is defined by

$$b(I_1) = \frac{1}{4\lambda}\left\{ \exp\left[-\xi(\lambda)\sqrt{I_1 - 3} \right] + \frac{\sinh[\nu(\lambda)(I_1 - 3)]}{\nu(\lambda)(I_1 - 3) + 1} \right\} \qquad (5)$$

where ξ(λ) and ν(λ) are adjustable parameters which it is possible to change with the relaxation time, λ.

Modified Leonov model has been used to fit all rheological data by using relaxation spectrum, flow activation energy and particular non-linear model parameters which are summarized in Tables 2-4. As it can been seen in Figures 1-3, modified Leonov model has excellent capability to describe rheological data for all tested polymer samples which fully justify the use this model in the theoretical flow analysis. The Figure 4 compares the differences between FCS1 and FCS2 sample. Clearly, even if the flow behavior in the shear flow is very similar, the extensional viscosity of both samples differs significantly. In more detail, the sample FCS2 is more extensional strain hardening than the FCS1 sample.

Results and discussion

Theoretical coextrusion flow analysis has been performed for two different feedblock geometries which are depicted in Figures 5-6 for processing conditions, which are summarized in Table 1. It should be mentioned that in this work, the finite element mesh with increased element density along the interfaces was used with the aim to reduce possible interpolation errors in the stress field along the interfaces (see Figures 7-8). Theoretical calculations have been performed for all processing conditions provided in Table 1 and the results are depicted in Figures 9-12. Interfacial stability analysis has been performed by quantifying the level of the stretching along the interfaces which has been found in past to be critical parameter for determining the onset of wave type of interfacial instabilities in multi manifold/film blowing dies [2-12]. In more detail, the quantification of the stretching (flow direction normal stress) discontinuity at the interface has been performed here by using Flow Direction Normal Stress Difference FDNSD variable, which is defined as following:

$$\mathrm{FDNSD} = \tau_{tt,1} - \tau_{tt,2} \qquad (6)$$

Where $\tau_{tt,1}$ is the flow direction normal stress locally on the interface from one side and $\tau_{tt,2}$ is the flow direction normal stress locally on the interface from another side. Note that FDNSD is calculated in one interface point and thus it quantifies the level and character of the stretching discontinuity just on the interface. The time dependent FDNSD has been calculated for all considered processing conditions and the results are depicted for each particular case in Figures 10 and 12 (for the FCS1/FCC and FCS2/FCC interfaces). As it can be seen, in some cases, the FDNSD takes positive sign only (Runs #1, #4 and #5 – Figures 10c, 12b and 12c), whereas in another cases the FDNSD change the sign significantly with the time (Runs #8, #2 – Figures 10b, 12a) or FDNSD change the sign just very slightly within extremely short time (Run #9 – Figure 10a). Note that FDNSD is very similar to Total Normal Stress Difference (TNSD) variable which was found to be sensitive enough to predict the onset of the interfacial instabilities for coextrusion of the same/different materials in multimanifold/film blowing dies [2-12] through the quantification of the sign changes in TNSD along the interface (unstable onset was related to the case when TNSD was changing the sign along the interface). If it is assumed here, that the mechanism for the wave type of interfacial instabilities is similar as described in [2-12], we can consider that flow become unstable also in the feedblock coextrusion flow domain when FDNSD change the sign on the interface. Based on this, it is possible to theoretically predict, whether the particular coextrusion flow condition is stable, unstable or stable/unstable. The comparison between experimentally and theoretically determined stability statuses is provided in Table 5. As it can be seen, the agreement between theoretical predictions and experimental data is very good.

Based on Table 5, it can also be concluded that the use of the FCS2 in the multilayer flow leads to much more unstable flow from the interfacial instabilities point of view than the use of the FCS1. This can be explained by the significantly higher extensional viscosity of FCS2 sample in contrary to FCS1 sample as shown in Figure 4.

Conclusion

- It has been found that the onset of the interfacial instabilities can be captured by the quantification of the stretching discontinuity occurring at the interface between different polymers through the sign change of the FDNSD.
- It has been revealed that the FCS2/FCC interface is much more sensitive to the interfacial instability onset than FCS1/FCC interface because the much higher FCS2 extensional viscosity in comparison to FCS1.

Acknowledgements: This work has been supported by Grant Agency of the Czech Republic, Grant No. 103/09/2066.

References

1. J. Dooley in S.G. Hatzikiriakos and K.B. Migler (Eds.), Polymer Processing Instabilities – Control and Understanding, Marcel Deeker, New York, 2005.
2. M. Zatloukal, C. Tzoganakis, J. Vlcek, P. Saha, International Polymer Processing, 16: (2), 198 (2001).
3. M. Zatloukal, J. Vlcek, C. Tzoganakis, P. Saha, Polymer Engineering and Science, 42: (7), 1520 (2002).
4. M. Zatloukal, W. Kopytko, A. Lengalova, J. Vlcek, Journal of Applied Polymer Science, 98, 153 (2005).
5. M. Martyn, R. Spares, P. Coates, M. Zatloukal, Journal of Non-Newtonian Fluid Mechanics, 156(3), 150 (2009).
6. M.T. Martyn, R. Spares, P.D Coates and M. Zatloukal, Plast. Rubber Comp., 33(1), 27 (2004).
7. M. Zatloukal., J. De Witte, Plastics Rubber and Composites 35(4), 149 (2006).
8. M. Zatloukal, W. Kopytko, P. Saha, M. Martyn., Plastics Rubber and Composites 34(9), 403 (2005).
9. M. Zatloukal, M.T. Martyn, P.D. Coates, J. Vlcek, Plastics Rubber and Composites 33(7), 305, (2004).
10. M. Zatloukal, J. Vlček, C. Tzoganakis, P.Sáha, SPE Antec papers, 44, (2001).
11. M. Zatloukal, J. Vlček, C. Tzoganakis, P.Sáha., TAPPI, San Diego, Canada (2001).
12. M. Zatloukal, M.T. Martyn, P.D. Coates, J. Vlcek, Plastics Rubber and Composites 33 (7): 305-309, (2004).
13. Sentmanat M.L., Rheol. Acta 43, 657 (2004).
14. Sentmanat M.L., Wang B.N., MCKinley G.H., J. Rheol. 49, 585 (2005).
15. Leonov A.I., Rheol. Acta 15, 85 (1976).
16. Zatloukal M., J. Non-Newtonian Fluid Mech. 113, 209 (2003).

Key Words: Coextrusion, Interfacial instabilities, Feedblock Coextrusion die.

Table 1: Experimental conditions for particular coextrusion runs in two different Feedblock dies (melt temperature was 450F in all layers).

		Extruder A		Extruder B		Extruder C		Extruder D		Extruder E	
Run #	Feedblock	Resin	Phr	Resin	phr	Resin	phr	Resin	phr	Resin	phr
1	New	FCS2	18.5	FCC	25.5	FCC	190.3	FCC	28.3	FCS2	17.4
2	New	FCS2	42.8	FCC	8.0	FCC	194.0	FCC	8.7	FCS2	42.3
4	New	FCS1	27.5	FCC	21.0	FCC	193.7	FCC	23.2	FCS1	26.4
5	New	FCS1	18.5	FCC	25.5	FCC	190.3	FCC	28.3	FCS1	17.4
8	Original	FCS2	42.8	FCC	8.0	FCC	194.0	FCC	8.7	FCS2	42.3
9	Original	FCS1	42.8	FCC	8.0	FCC	194.0	FCC	8.7	FCS1	42.3

Table 2: Modified Leonov model parameters for *FCC sample* (reference temperature Tr=235°C, flow activation energy Ea=28.6 kJ/mol).

	Maxwell parameters		mLeonov model	
i	$\lambda_{b,i}$ [s]	G_i [Pa]	ξ	ν
1	0.001	95841.438	0	0
2	0.01	37228.965	0	0.1
3	0.1	13143.549	0	0.1
4	1	2146.657	0.245	0.0024
5	10	200.958	0.04	0.001
6	100	11.516	0	0.001
7	1000	0.823	0	0.01

Table 3: Modified Leonov model parameters for *FCS1 sample* (reference temperature Tr=235°C, flow activation energy Ea=44.3 kJ/mol).

	Maxwell parameters		mLeonov model	
i	$\lambda_{b,i}$ [s]	G_i [Pa]	ξ	ν
1	0.001	67289.21	0.25	0.02
2	0.01	21448.62	0.25	0.02
3	0.1	8026.521	0.25	0.04
4	1	1312.508	0.3	0.055
5	10	108.296	0	0.05
6	100	5.249	0	0.06
7	1000	0.298	0	0.08

Table 4: Modified Leonov model parameters for *FCS2 sample* (reference temperature Tr=235°C, flow activation energy Ea=41.7 kJ/mol).

	Maxwell parameters		mLeonov model	
i	$\lambda_{b,i}$ [s]	G_i [Pa]	ξ	ν
1	0.001	78550.6	0	0.5
2	0.01	23544.24	0	0.5
3	0.1	7012.738	0	0.5
4	1	1013.927	0	0.5
5	10	94.494	0.09	0.000022
6	100	5.507	0.0397	0.000085
7	1000	0.424	0.012	0.00001

Table 5: Experimentally and theoretically determined coextrusion stability for different processing conditions which are provided in Table 1.

Run #	Feedblock	Stability - experiment	Stability - simulation
1	New	Stable	Stable
2	New	Unstable	Unstable
4	New	Stable	Stable
5	New	Stable	Stable
8	Original	Highly Unstable	Unstable
9	Original	Just Stable	Stable/Unstable

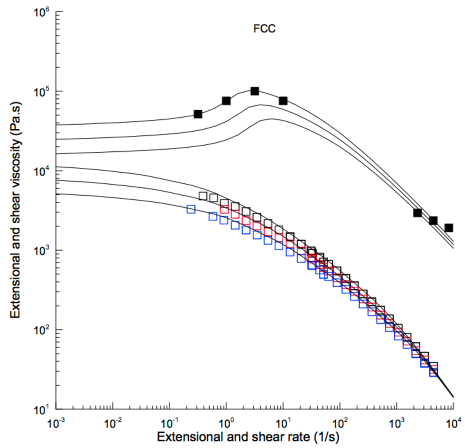

Figure 1: Comparison between modified Leonov model predictions (lines) and experimentally determined shear (open squares) and extensional (full squares) viscosities at 215°C (black symbols), 235°C (red symbols) and 255°C (blue symbols) for sample FCC.

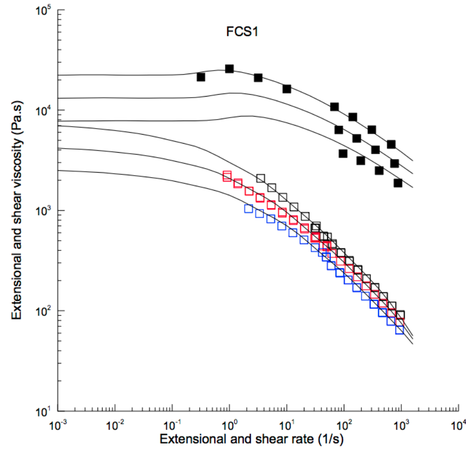

Figure 2: Comparison between modified Leonov model predictions (lines) and experimentally determined shear (open squares) and extensional (full squares) viscosities at 215°C (black symbols), 235°C (red symbols) and 255°C (blue symbols) for sample FCS1.

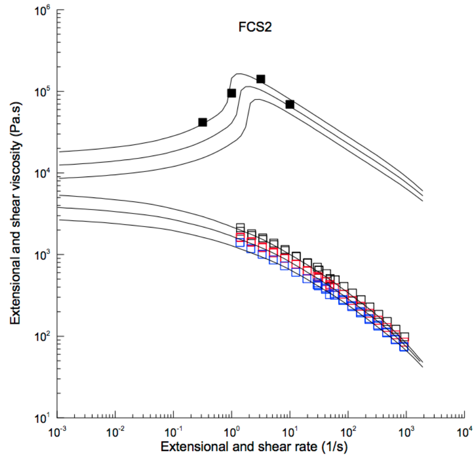

Figure 3: Comparison between modified Leonov model predictions (lines) and experimentally determined shear (open squares) and extensional (full squares) viscosities at 215°C (black symbols), 235°C (red symbols) and 255°C (blue symbols) for sample FCS2.

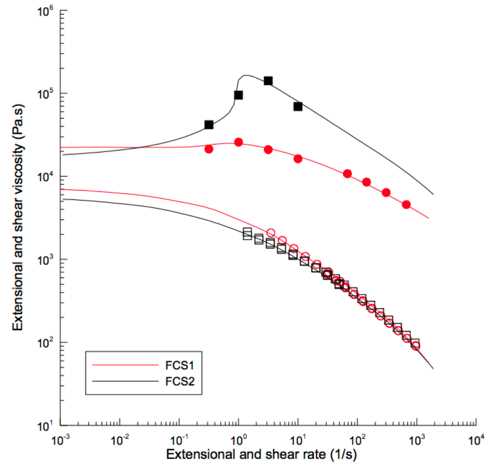

Figure 4: Comparison between shear (open symbols) and extensional (full symbols) viscosities for samples FCS1 (red color) and FCS2 (black color) at 215°C. Lines represent modified Leonov model fit.

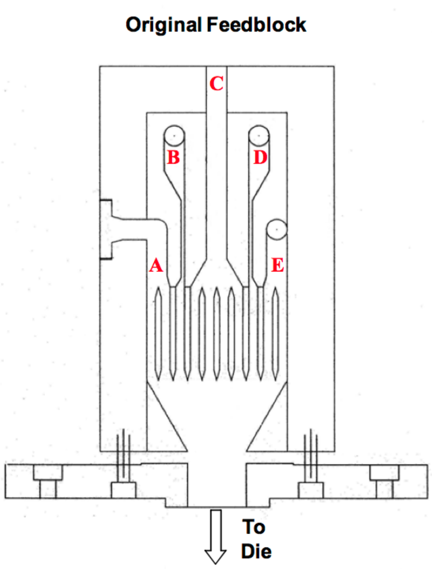

Figure 5: Sketch of the original feedblock geometry.

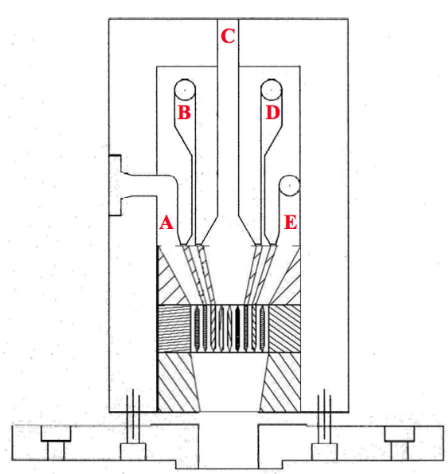

Figure 6: Sketch of the New (modified) feedblock geometry. In more detail, the flow channel of the original feedblock has been reduced with inserts of dimensions (in inches) shown in Figure 5 whereas the width stayed the same.

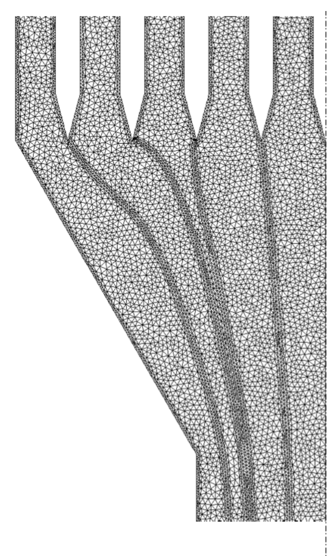

Figure 7: FEM mesh with increased element density along the interfaces (Run #8).

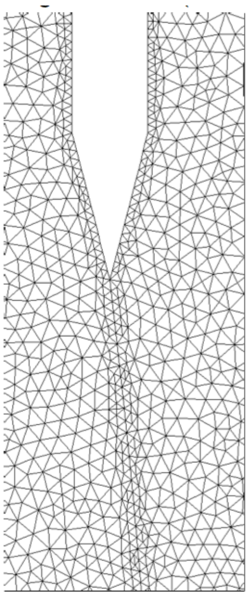

Figure 8: Detail view of the FEM mesh with increased element density along the interfaces (Run #8).

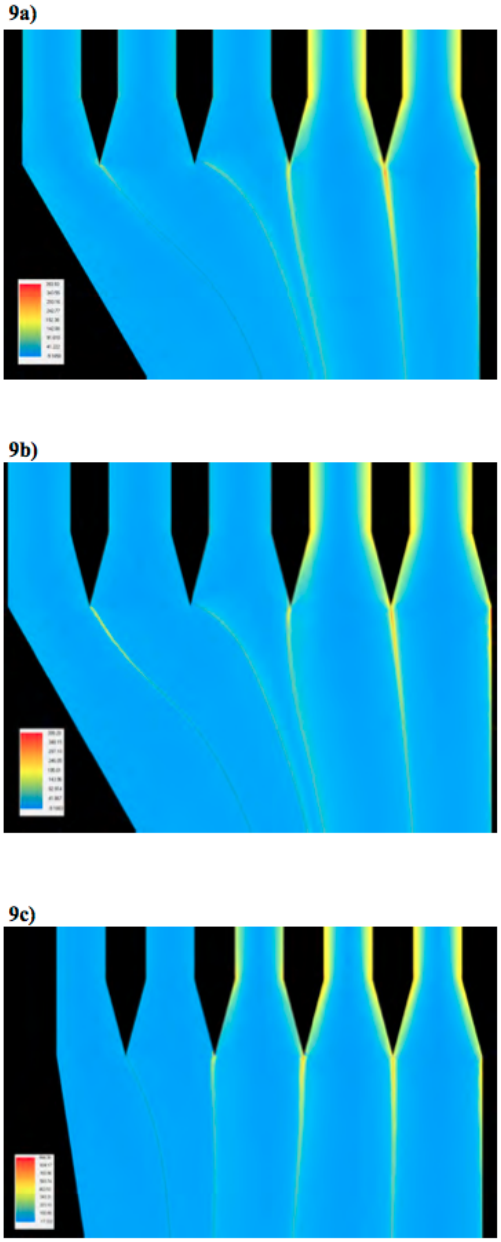

Figure 9: Detail view of calculated local flow direction normal stress field at the merging area for different runs.
9a) Run #9 (Stable/Unstable).
9b) Run #8 (Highly Unstable).
9c) Run #1 (Stable).

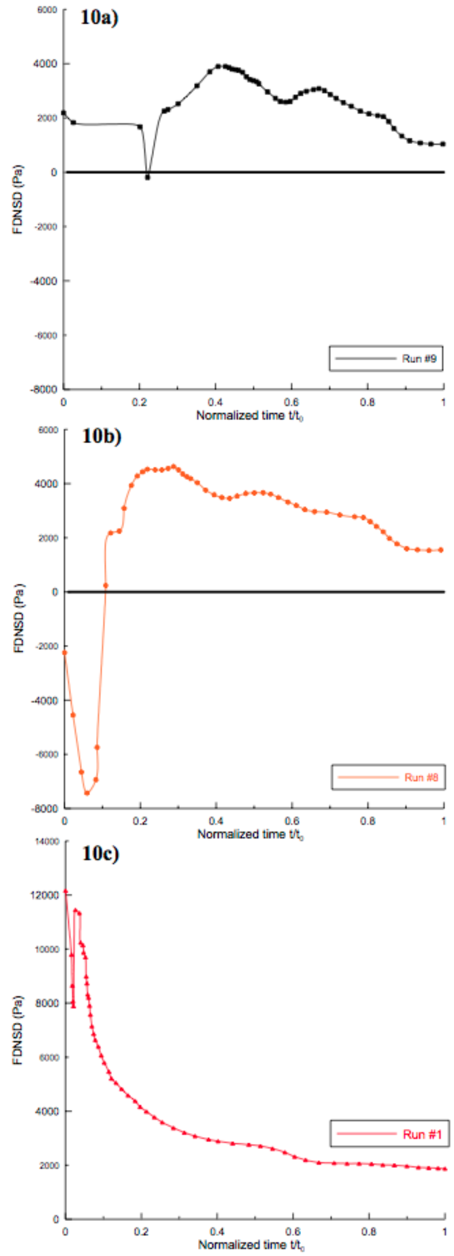

Figure 10: Local Flow Direction Normal Stress Difference (FDNSD) at the FCS2/FCC interface as the function of the normalized residence time for different runs. **10a)** Run #9; **10b)** Run #8; **10c)** Run #1.

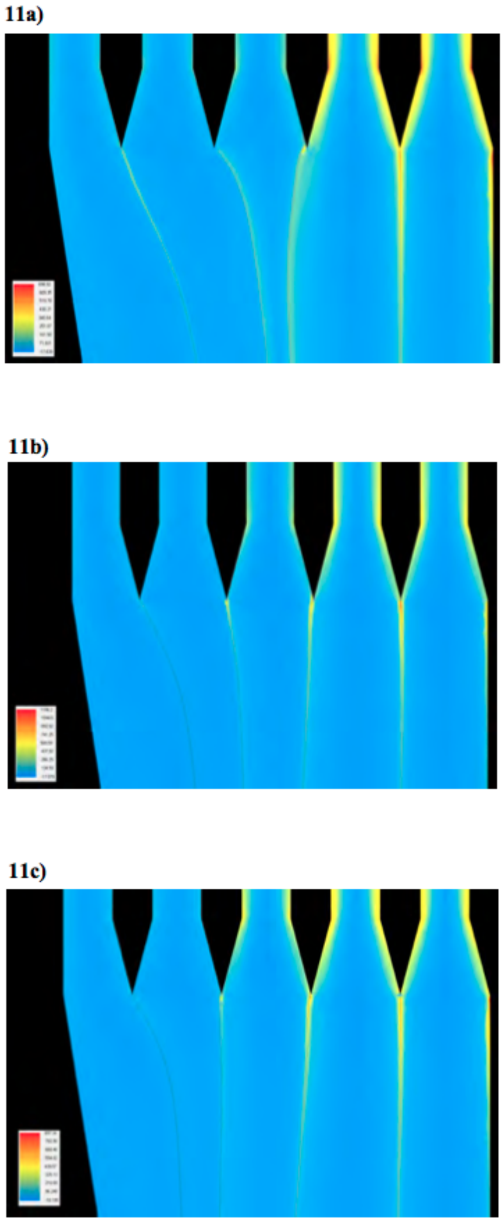

Figure 11: Detail view of calculated local flow direction normal stress field at the merging area for different runs.
11a) Run #2 (Unstable).
11b) Run #4 (Stable).
11c) Run #5 (Stable).

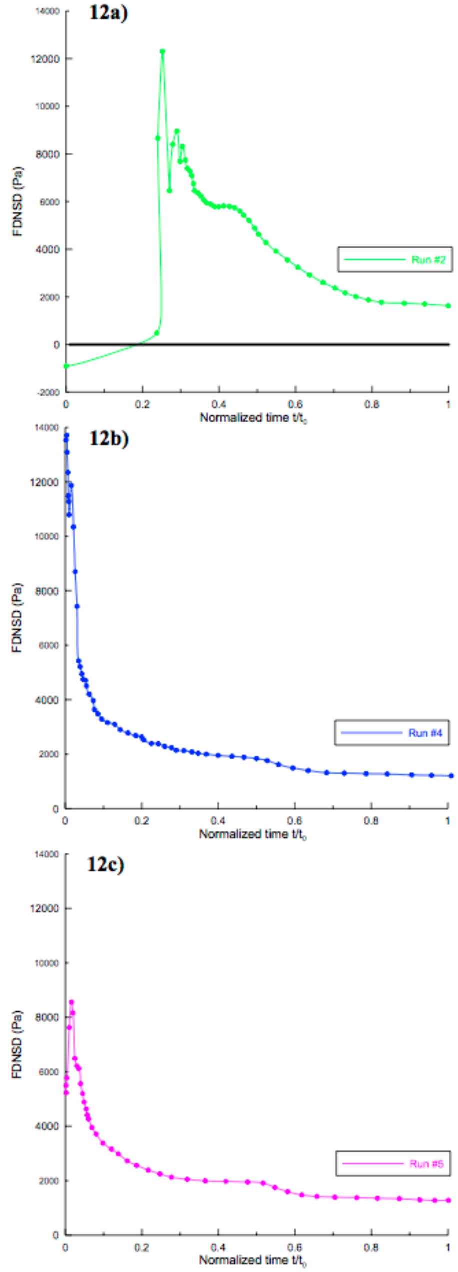

Figure 12: Local Flow Direction Normal Stress Difference (FDNSD) at the FCS2/FCC interface as the function of the normalized residence time for different runs. **12a)** Run #2; **12b)** Run #4; **12c)** Run #5.

Return to Paper of the Month.